

1 Nonlinear X Waves

CLAUDIO CONTI⁽¹⁾ and STEFANO TRILLO⁽²⁾

(1) Research center “Enrico Fermi,” Via Panisperna 89/A, 00100 Roma, Italy and Research center SOFT INFM-CNR, University “La Sapienza,” P.le Aldo 5, 00185 Roma, Italy

(2) Dipartimento di Ingegneria, University of Ferrara, Via Saragat 1, 00144 Ferrara

... to kill that savage monster, the Chimaera, who was not a human being, but a goddess, for she had the head of a lion and the tail of a serpent, while her body was that of a goat, and she breathed forth flames of fire ...

—(The Iliad, Book VI, translated by Samuel Butler)

1.1 INTRODUCTION

A non-monochromatic superposition of propagation-invariant beams is obviously a propagation-invariant beam itself. However this is no longer the case when the superposition principle ceases to be valid, as in the case of wave propagation in nonlinear media. On the other hand it is well known that the nonlinearity can counteract beam spreading, being at the very origin of those strongly confined propagation-invariant wave-packets that are known as solitons or solitary waves (SW) [1, 2]. Unfortunately, SW typically involve a reduced number of dimensions, whereas the observation of a three dimensional (3D) SW has been elusive to date [3, 4]. Among various reasons behind this, the most relevant are: (i) the fact that 3D-SW are affected by intrinsic instabilities; (ii) (more specific to optics) 3D-SW not only require a nonlinear medium (and hence very high laser intensities) but also anomalous material dispersion (i.e., $k'' \equiv d^2k/d\omega^2 < 0$ where k is the wave-number).

In contrast with SW, localized waves (LW) are 3D propagation-invariant wave-packets that do not rely on any nonlinearity. They have been observed in several contexts (see the other contributions to this book) and in principle they should not exist in a nonlinear medium since they rely on the superposition principle. In this respect the experimental observation of optical 3D propagation-invariant pulses, so-called “light bullets”, in a nonlinear medium

with normal dispersion ($k'' > 0$), i.e. in a regime where both LW and SW were not expected to exist, did really appear as an astonishing result [5, 6]. The spatio-temporal far-field spectrum of the observed light bullets clearly appeared as an “X” [7], and an accurate and sophisticated experimental reconstruction (“tomography”) of the spatio-temporal profile unveiled the double conical structure of the wave-packet [8, 9] in agreement with theoretical and numerical analysis [10, 11, 12, 13, 14, 15, 16]. Thus, naturally, the light bullet was dubbed “nonlinear X-wave”. This result opened many different roads of investigations, mainly aimed at providing for a physical and mathematical background to a special class of nonlinear 3D beams whose features recall both SW (they spontaneously form at high intensity and propagate without sensible distortion) and linear LW (the structure is seemingly that of conical waves), thus constituting a sort of *Chimaera*.

Thereafter the field of nonlinear X-waves (NLX) has rapidly grown, on one hand linking linear LW solutions in dispersive media to the existing literature and the plethora of electromagnetic LW mainly investigated as solutions of Maxwell’s equations in vacuum (see other chapters in this book) [17, 18, 19, 20, 21, 22, 23, 24, 25, 26, 27, 28, 29] and, on the other hand, attempting to extend the idea of “non-bell-shaped” localized solutions to the very active field of nonlinear optics which deals with solitary waves, including periodic media and different kind of nonlinearities [30, 31, 32, 33, 34, 35, 36, 37, 38, 39, 40, 41, 42, 43, 44, 45, 46, 47]. Importantly, numerical simulations, experiments and theory concurred to establish that NLX can be also an effective paradigm for interpreting ultra-fast laser propagation in nonlinear media with an intensity dependent refractive index (i.e., “Kerr media”). Given the facts that any material displays such a nonlinearity at sufficiently high intensities, and that many experiments have been done in water or air (due to virtual absence of damage threshold), these results have many implications in bio-physical or remote environmental sensing applications [48, 15, 16, 49, 50, 51, 52, 53, 54, 55, 56].

Moreover, the formal analogy between nonlinear optics in Kerr media and time-evolution of the semi-classical wave-function of ultra-cold bosons has led to the prediction of the existence of “Matter X-waves” [57]. Matter waves are a natural manifestation of large scale coherence of an ensemble of atoms populating a fundamental quantum state. The observation of Bose-Einstein condensates (BECs) in dilute ultra-cold alkalis [58, 59] has initiated the exploration of many intriguing properties of matter waves, whose macroscopic behavior can be successfully described via mean-field approach in terms of a single complex wave-function [60]. Large scale coherence effects are usually observed by means of 3D magnetic or optical confining potentials in which BECs are described by their ground-state wave-function. Trapping can also occur in free space (i.e. without a trap) through the mutual compensation of the leading-order (namely, two-body) interaction potential and kinetic energy, leading to matter-SW. This phenomenon, however, has been observed only in 1D [61]. In 2D and 3D, free-space localization cannot occur due to mentioned

instability of SW, and even in a trap collapse usually prevents stable formation of BEC [62, 63], needing stabilizing mechanisms [64]. For these reasons, the use of periodic potentials induced by optical *lattices* [65], where the behavior of atoms mimics that of electrons in crystals or photons in periodic media [66, 67] is attracting a great deal of interest: for instance, in 1D (elongated) lattices 1D-SW can form and are referred to as “gap solitons” [68]. Notably enough, in the presence of a 1D lattice potential, the 3D dynamics of the fundamental state wave-function formally obeys to the same model of NLX in optics. Specifically, under conditions for which the Bloch state associated with the lattice has a negative effective mass, the natural state of BECs is a localized *matter X wave* characterized by a peculiar bi-conical shape. The atoms are organized in this way in the absence of any trap, solely as the result of the strong anisotropy between the 1D periodic modulation and the free-motion in the 2D transverse plane. In this respect, NLX appear as novel non-trivial localized states of ultra-cold atoms.

This chapter is aimed at reviewing many of the aforementioned aspects of NLX. A strong emphasis is given to the theory and especially to “X-wave oriented” analytical techniques that directly involve LW in the nonlinear dynamics. This approach has to be compared with plane-wave oriented approaches. Given the fact that many of the well known classifications of LW (detailed in this book) lose their meaning when dealing with nonlinear effects, we will roughly indicate with “X-waves” those solutions whose intensity profile travels undistorted, thus using LW and X-waves as synonymous.

Outline. In section 1.2 we review the basic models for nonlinear optical propagation and BEC; in section 1.3 we introduce *envelope X-waves*, i.e. linear X-waves in the paraxial and slowly varying envelope approximation (SVEA) and the corresponding X-wave expansion that leads to finite energy solutions; section 1.4 is devoted to discuss how nonlinear processes foster the exponential amplification of LW at the expense of a pump beam; in section 1.5 we apply the X-wave expansion to derive general results for the nonlinear propagation and generation of LW; section 1.6 deals with numerical results concerning the exact profile of X-waves in nonlinear media; in section 1.7 we discuss an approach to the highly nonlinear dynamical processes observed in experiments: the *coupled X-wave theory*; section 1.8 contains a brief review of experimental results, while conclusion and perspectives are drawn in section 1.9.

1.2 THE NLX MODEL

The reference model for NLX pertains to a medium where the nonlinearity is responsible for a direct self-action on a wave-packet envelope. In nonlinear optics, self-action occurs typically through a third-order effect (the dielectric polarization depends on the electric field cube) that involves degenerate four-photon mixing interactions $\omega = \omega - \omega + \omega$ among photons at the generic

frequency ω within the bandwidth of the field. This is well known to be equivalent to a refractive index varying according to the Kerr law $n(\omega) = n_0(\omega) + n_{2I}I$ where $n_0(\omega)$ is the linear or low-intensity index, I is the optical intensity and n_{2I} is known as the Kerr nonlinear index coefficient. In such a medium, under standard approximations (paraxial and SVEA), an electric field with linearly polarized unit vector \mathbf{e} and a spatio-temporal spectrum localized around the propagation direction $(k_x, k_y, k_z) = (0, 0, k) \equiv \mathbf{k}$ and vacuum carrier wavelength $\lambda = 2\pi c/\omega_0$,

$$\mathbf{E} = \Re \left[\mathbf{e} \sqrt{\frac{2Z_0}{n(\omega)}} A(\mathbf{r}, T) \exp(ikz - i\omega_0 T) \right], \quad (1.1)$$

has its complex electric field envelope A obeying the equation (see e.g. [69])

$$i \frac{\partial A}{\partial z} + ik' \frac{\partial A}{\partial T} - \frac{k''}{2} \frac{\partial^2 A}{\partial T^2} + \frac{1}{2k} \nabla_{\perp}^2 A = -k_0 n_{2I} |A|^2 A, \quad (1.2)$$

where $\nabla_{\perp}^2 \equiv \partial_x^2 + \partial_y^2$, $k = k_0 n_0 = \omega_0 n_0 / c$ is the wave-number at carrier angular frequency ω_0 , and the prime denotes the derivative with respect to ω calculated at ω_0 . Note that the square root containing the vacuum impedance Z_0 in Eq. (1.1) is such that the square modulus of the envelope gives directly the intensity, i.e. $I = |A|^2$.

Although in this chapter we mainly restrict to the model (1.2), we observe that its validity extends well beyond Kerr media and even nonlinear optics (as discussed below it is also approximately valid for a quadratically nonlinear medium and, within a perturbative formulation, when dealing with ultra-cold gases). We point out that, even in the case of Kerr media (and within paraxial-SVEA), it does not take into account many phenomena that are expected and observed when dealing with the propagation of femtosecond-pulses in water or air, such as those related to plasma-formation or higher order dispersion. Although many generalizations of the models and the exploration of the related issues, are indeed possible within the paradigms of LW, Eq. (1.2) is very rich and describes the essential physics of LW, thus appearing as the most relevant basic model for NLX.

Quadratic media and second harmonic generation As mentioned in the introduction, media for the second harmonic generation (SHG) are relevant for NLX, because they were employed in the first experimental demonstration [12]. In the most general case the nonlinear interaction in a quadratically nonlinear medium [i.e. a medium in which any component of the nonlinear polarization is expressed in terms of the products of two electric field components] commits together three optical carriers ω_i ($i = 1, 2, 3$) such that $\omega_3 = \omega_1 + \omega_2$. At variance with Kerr media, where only one angular frequency is involved, the model is given by three coupled envelope equations of the kind of Eq. (1.2). For the partially degenerate case of SHG, when $\omega_1 = \omega_2 = \omega$

and $\omega_3 = 2\omega$, only two equations have to be considered, as reported in the literature (see [11, 13, 14, 30, 70]). However, in this manuscript, we will restrict ourselves to Kerr media, while recalling that in suitable regimes Eq. (1.2) is a good approximation for the nonlinear dynamics of the fundamental beam at ω also in quadratic media (see e.g. [1]).

Bose-Einstein condensation. In the presence of a lattice, the Gross-Pitaevskii equation models the mean-field dynamics of ultra-cold boson (see e.g. [60]). As discussed in more detail in Ref. [57], in the presence of an external lattice (which can be induced on the atom cloud by the interference of counter-propagating laser beams), the Gross-Pitaevskii equation reduces to an equation similar to Eq. (1.2):

$$i\hbar\partial_t\phi + \frac{\hbar^2}{2m} \left(\nabla_{\perp}^2 - \frac{m}{m_e} \partial_z^2 \right) \phi - \frac{3a}{2} |\phi|^2 \phi = 0, \quad (1.3)$$

where m and a are the boson mass and the “scattering length”, respectively, and m_e is the negative effective mass, which depends on the lattice period and the strength of the corresponding potential, as experimentally investigated in [71]. A *matter X wave*, solution of Eq. (1.3) as detailed below, entails localization in both momentum and configuration space, thus being a clear signature of a Bose condensed gas, so much as the anisotropy in the distribution function detected in early experiments [60]. Unlike any other form of BEC including solitons, matter X waves can be observed in free-space and in non-interacting regime, where they are the natural basis to describe the coherent properties of atom wave-packets. In order to fix the notation, we will make explicit reference to optics in the following, where experimental evidences have already been reported. The results for the BEC are obtained via the formal substitution: $A \rightarrow \phi$, $z \rightarrow t$, $T \rightarrow z$, $k' \rightarrow 0$, $k'' \rightarrow \hbar/m_e$, $k \rightarrow m/\hbar$, $k_0 n_{2I} \rightarrow 3a/2\hbar$.

1.3 ENVELOPE LINEAR X-WAVES

Envelope X-waves are linear X-waves in the paraxial slowly-varying envelope approximation, or in other words solutions of our model (1.2) in the limit of zero intensity ($n_{2I} = 0$), that reads explicitly as

$$i\partial_z A + ik'\partial_T A - \frac{k''}{2} \partial_T^2 A + \frac{1}{2k} \nabla_{\perp}^2 A = 0. \quad (1.4)$$

The case of interest here is that of normal dispersion $k'' > 0$ yielding a hyperbolic operator. Eq. (1.4) can be further simplified by introducing the retarded

time $t \equiv T - k'z$, so that Eq. (1.4) can be rewritten as

$$i\partial_z A - \frac{k''}{2}\partial_t^2 A + \frac{1}{2k}\nabla_\perp^2 A = 0. \quad (1.5)$$

Looking for “stationary solutions” (i.e., solutions traveling with natural group velocity $1/k'$, such that $\partial_z = 0$ in Eq. (1.6)) yields an equation which is formally identical to the one obtained from the scalar wave-equation when considering standard LW:

$$\nabla_\perp^2 A - k k'' \partial_t^2 A = 0. \quad (1.6)$$

Thus all the solutions which are known from the theory of LW in vacuum gives corresponding envelope X-wave solutions. More general axi-symmetric envelope X-waves can be sought for in the form

$$A = \psi(t - \beta z, r) \exp(ik_z z), \quad (1.7)$$

which corresponds to an intensity profile $I = |A|^2$ traveling as an invariant object in the z -direction with group velocity $(1/k' + 1/\beta)^{-1}$ measured in the laboratory frame. In the case $k' = 0$ (e.g., for BEC waves) these solutions represent still 3D bullets. Introducing a retarded time $t_\beta \equiv t - \beta z$, the equation for ψ reads as

$$-k_z \psi - i\beta \partial_{t_\beta} \psi - \frac{k''}{2} \partial_{t_\beta}^2 \psi + \frac{1}{2k} \nabla_\perp^2 \psi = 0, \quad (1.8)$$

Let ψ a superposition of monochromatic Bessel beams, $J_0(\sqrt{k k''} \alpha r) \exp(-i\omega t_\beta)$, with α in frequency units, the corresponding spatio-temporal dispersion relation is

$$-k_z - \beta\omega + \frac{k''}{2}\omega^2 = \frac{k''\alpha^2}{2}. \quad (1.9)$$

In order to have a continuous spectrum along ω , the left-hand side must be positive, thus ensuring the absence of evanescent waves. This can be achieved, in the simplest way, by letting $k_z = -\beta^2/2k''$, which gives

$$\left(\omega - \frac{\beta}{k''}\right)^2 = \alpha^2. \quad (1.10)$$

Equation (1.10) implies the existence of two types of X-waves that parametrically depend on the inverse velocity β

$$\begin{aligned} \psi_+(t_\beta, r; \beta) &= \int_0^\infty e^{-i(\frac{\beta}{k''} + \alpha)t_\beta} J_0(\sqrt{k'' k} \alpha r) f_+(\alpha) d\alpha, \\ \psi_-(t_\beta, r; \beta) &= \int_0^\infty e^{-i(\frac{\beta}{k''} - \alpha)t_\beta} J_0(\sqrt{k'' k} \alpha r) f_-(\alpha) d\alpha, \end{aligned} \quad (1.11)$$

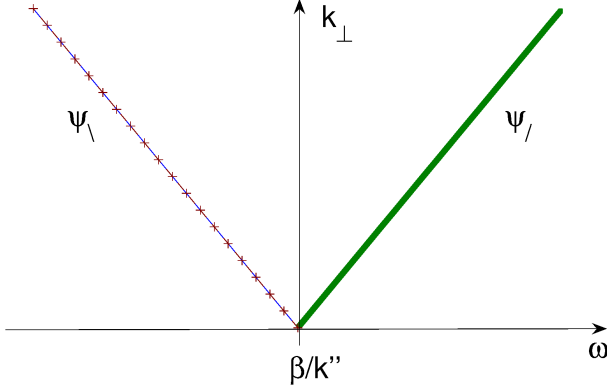


Fig. 1.1 Sketch of spatio-temporal spectra of “slash” and “backslash” X-waves.

with the corresponding “spectra” $f_{/}(\alpha)$ and $f_{\backslash}(\alpha)$. They will be denoted as “slash” and “backslash” X-waves, because of the shape of their spatio-temporal frequency content, as discussed below. A general linear X-wave solution characterized by the inverse differential velocity β is given by

$$A_X = e^{-i\frac{\beta^2}{2k''}z} [\psi_{/}(t - \beta z, r; \beta) + \psi_{\backslash}(t - \beta z, r; \beta)], \quad (1.12)$$

which can be rewritten as

$$A_X = e^{-i\frac{\beta}{k''}t + i\frac{\beta^2}{2k''}z} [\varphi_{/}(t - \beta z, r) + \varphi_{\backslash}(t - \beta z, r)], \quad (1.13)$$

with

$$\varphi_X(t_\beta, r) = \int_0^\infty e^{\mp i\alpha t_\beta} J_0(\sqrt{k''k\alpha r}) f_X(\alpha) d\alpha. \quad (1.14)$$

Here the “X” stands for either / or \backslash , and φ_X corresponds to X-waves of the scalar wave equation (see e.g. Ref. [72] or the other chapters of this book). Note that f_X is complex-valued. The spatio-temporal spectrum of $A_X(r, t, z)$, is centered at the shifted central frequency β/k'' , determined by the X-wave velocity, and it looks like an “X” in the angle-frequency plane, as shown in figure 1.1 for $k_\perp > 0$ (positive angles). The following relation holds useful for any $\psi_X(t - \beta z, r; \beta)$:

$$\mathcal{L}\psi_X \equiv \left(i\partial_z + \frac{1}{2k} \nabla_\perp^2 - \frac{k''}{2} \partial_t^2 \right) \psi_X = -\frac{\beta^2}{2k''} \psi_X. \quad (1.15)$$

Therefore an X-wave can also be defined as a solution of Eq. (1.6) of the type $A_X = C(z, \beta)\psi_X(t - \beta z, r)$ with C obeying the equation

$$i\frac{\partial C}{\partial z} - \frac{\beta^2}{2k''} C = 0, \quad (1.16)$$

which turns out to be a useful information when one formulates a nonlinear approach.

The invariant envelope X-waves contain, in general, an infinite energy. This is due to the idealized situation (never achieved in experiments) of a precisely defined velocity (or inverse differential velocity β). Any finiteness introduced by the experimental setup, as e.g. the spatial extension of the sample, will in general fade the spectrum line-shape around the X, determining uncertainty in β . In the following, we will show how to introduce a packet of X-waves, with velocities around a given value and finite energy. Considering an X-wave with a specific velocity is as idealized as considering an elementary particle of given momentum.

1.3.1 X-wave expansion and finite energy solutions

The X-wave transform. The general solution of Eq. (1.4) can be expressed by the Fourier-Bessel spectrum of the field at $z = 0$, denoted by $S(\omega, k_{\perp}) = \mathcal{B}[A](\omega, k_{\perp}, 0)$:

$$A(r, z, t) = \int_0^{\infty} \int_{-\infty}^{\infty} S(\omega, k_{\perp}) J_0(k_{\perp} r) e^{i(k_z z - \omega t)} k_{\perp} dk_{\perp} d\omega, \quad (1.17)$$

with $k_z = -k_{\perp}^2/2k + k''\omega^2/2$. By a simple variable change, the field can be written as a superposition of slash-X-waves, traveling with different velocities. If we set

$$\omega = \alpha + \frac{\beta}{k''}; \quad k_{\perp} = \sqrt{k k''} \alpha \quad (1.18)$$

we obtain that

$$A(r, z, t) = \int_{-\infty}^{\infty} e^{-i \frac{\beta^2}{2k''} z} \Psi_{/}(t - \beta z, r; \beta) d\beta, \quad (1.19)$$

while being

$$\Psi_{/}(t - \beta z, r; \beta) = \int_0^{\infty} X_{/}(\alpha, \beta) J_0(\sqrt{k k''} \alpha r) e^{-i(\alpha + \frac{\beta}{k''})(t - \beta z)} d\alpha, \quad (1.20)$$

and

$$X_{/}(\alpha, \beta) \equiv \mathcal{X}_{/}[A(r, t, z = 0)](\alpha, \beta) \equiv k \alpha S \left(\alpha + \frac{\beta}{k''}, \sqrt{k k''} \alpha \right). \quad (1.21)$$

An equivalent representation is obtained by backslash-X-waves. The variable change (1.18) corresponds to span the (ω, k_{\perp}) space by oblique (slash) parallel lines in (1.17). Eq. (1.20) is a formulation of the ‘‘X-wave transform’’, first introduced in Ref. [73] and indicated as $\mathcal{X}[A](\alpha, \beta)$. Hence the spatio-temporal evolution due to the interplay of diffraction and dispersion, can be represented by one dimensional propagation of packets with different velocities.

Orthogonal X-waves and finite energy solutions. An arbitrary pulsed-beam can be expressed as a superposition of X-waves traveling with different velocities. Conversely, such a superposition can be used to construct new-classes of physically realizable finite-energy X-waves. To this extent, orthogonal X waves –first introduced in [74] for the wave equation– are a fruitful approach (see also [16]). With reference to two (either slash or backslash) X-wave solutions of Eq. (1.8), denoted by A_X and B_X , with inverse differential velocities β and β' and spectra f and g , respectively, the inner-product can be defined as the integral of $B_X^* A_X$ with respect to x, y, t , extended on the whole space. A specific class of spectra, denoted as f_p with $p = 0, 1, 2, \dots$, satisfies the orthogonality condition ($A_q = B_X$ and $A_p = A_X$) holds:

$$\langle A_q(r, t, z, \beta) | A_p(r, t, z, \beta') \rangle = \delta_{pq} \delta(\beta - \beta'). \quad (1.22)$$

When $X(\alpha, \beta) = C(\beta) f_p(\alpha)$, it is $\mathcal{E}_\beta = |C(\beta)|^2$, the resulting beam is a finite energy X-wave that spreads according to a prescribed velocity distribution function $C(\beta)$; this corresponds to the existence of solutions with an arbitrary “depth of focus”. This kind of wave-packet can be written, with reference to slash X-waves, as

$$A = \int_{-\infty}^{\infty} C(\beta, z) \psi_j^{(q)}(r, t - \beta z; \beta) d\beta, \quad (1.23)$$

with C obeying Eq. (1.16). Introducing a suitable Fourier transform with respect to the variable β

$$c(s, z) = \frac{1}{2\pi\sqrt{k''}} \int_{-\infty}^{\infty} C(\beta, z) e^{i\frac{\beta}{k''}s} d\beta, \quad (1.24)$$

we obtain, from Eq. (1.16), that c obeys the equation

$$i \frac{\partial c}{\partial z} + \frac{k''}{2} \frac{\partial^2 c}{\partial s^2} = 0. \quad (1.25)$$

Therefore the 3D linear propagation of an X-wave packet in a normally dispersive medium can be reduced to that of a 1D pulse with *anomalous* dispersion. The energy is

$$\mathcal{E} = 2\pi \int_0^{\infty} \int_{-\infty}^{\infty} |A(r, t, z)|^2 r dr dt = \int_{-\infty}^{\infty} |C(\beta)|^2 d\beta = 2\pi \int_{-\infty}^{\infty} |c(s)|^2 ds. \quad (1.26)$$

In the following the (slash) X-wave, with spectrum

$$f_0(\alpha) = \frac{\sqrt{k}}{\pi} \Delta \alpha \exp(-\Delta \alpha), \quad (1.27)$$

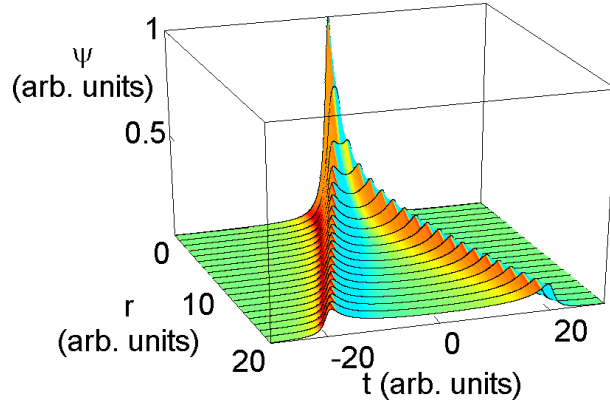


Fig. 1.2 Spatio-temporal profile of the fundamental X-wave (1.2).

and spatio-temporal profile

$$\varphi_{/}^{(0)} = -\frac{\sqrt{k}}{\pi} \frac{\Delta}{\left[1 - \frac{k k'' r^2}{(s - i\Delta)^2}\right]^{3/2} (s - i\Delta)^2}, \quad (1.28)$$

is the simplest X-wave with finite power (i.e. the integral of $|\varphi_{/}^{(0)}|^2$ over transverse variable converges, see also Ref. [21]). This X wave is shown in figure 1.2.

1.4 CONICAL EMISSION AND X-WAVE INSTABILITY

So far we dealt with linear X-waves of a simplified scalar model, prolegomena to the nonlinear regime. The fundamental physical result is that, in nonlinear media, X-waves are spontaneously generated during the propagation of a bell-shaped (in space and time) pulse. The universal mechanism of wave spectral reshaping in nonlinear media is the *modulational instability* (MI), which describes the amplification of plane-waves at the expense of a pump beam. The features of MI depends on the number of effective dimensions and the sign of dispersion; in the most general case, i.e. when a propagation coordinate z , two transverse coordinates x, y and time t are taken into account MI in a normally dispersive medium takes the name of *conical emission* (CE). CE describes a well known and experimentally investigated effect, namely the generation of far-field rings with different colors when a intense ultra-short pulse propagate in a nonlinear medium [75, 76, 77, 78, 55]. The analysis of CE is technically simple and relies on a linearized perturbative approach [11]. In the following, we will reformulate this treatment to see how X-waves can be directly involved [15]. First, we rewrite Eq. (1.2) in terms of dimensionless variables

by setting $u = A/\sqrt{I_0}$, $(\xi, \eta) = (x, y)/W_0$, $\zeta = z/Z_{df}$, $\tau = (t - k'z)/T_0$, $\Gamma = Z_{df}/Z_{nl}$, where I_0 is a reference intensity (e.g., the input beam peak intensity), W_0 is a reference waist (e.g., the input beam waist), $Z_{df} = 2kW_0^2$ and $Z_{nl} = (k_0 n_{2I} I)^{-1}$ are diffraction and nonlinear length scales, respectively, and $T_0 = (k''Z_{df}/2)^{1/2}$. The normalized equation reads as

$$i\partial_\zeta u + (\partial_\xi^2 + \partial_\eta^2) u - \partial_\tau^2 u + \Gamma|u|^2 u = 0. \quad (1.29)$$

Restricting ourselves to solutions traveling at the group velocity of the medium ($\beta = 0$), we consider X-waves $u = \psi(\xi, \eta, \zeta) \exp(i\kappa\zeta)$ in the linear case ($\Gamma = 0$), where ψ obeys the equation

$$(\partial_\xi^2 + \partial_\eta^2 - \partial_\tau^2) \psi = \kappa\psi. \quad (1.30)$$

Explicit solutions can be found for example by introducing the complex variable $v = (\Delta - i\tau)^2 + \xi^2 + \eta^2$, and looking for a solution $\psi = \psi(v)$ of the following equation

$$6\partial_v \psi + 4v\partial_{vv} \psi = \kappa\psi, \quad (1.31)$$

solved, e.g., the real valued solution (with parameters κ and Δ):

$$\psi_\kappa = \Re \left[\frac{\exp(-\sqrt{\kappa v})}{\sqrt{v}} \right]. \quad (1.32)$$

It is not difficult to recognize in Eq. (1.32) some of the well studied X-wave solutions for the scalar wave equation (see the other chapters in this book). Next, starting from the exact plane wave solution $u = u_0 \exp(iu_0^2 z)$ of Eq. (1.29), with u_0 a constant, the solution of the nonlinear wave equation is written as

$$u = [u_0 + \epsilon(\xi, \eta, \tau, \zeta)] \exp(iu_0^2 \zeta)$$

and, at the first order in the perturbation ϵ , the governing equation reads as

$$i\partial_\zeta \epsilon + \partial_\xi^2 \epsilon + \partial_\eta^2 \epsilon - \partial_\tau^2 \epsilon + \Gamma u_0^2 (\epsilon + \epsilon^*) = 0. \quad (1.33)$$

If we set $\epsilon = \mu(z)\psi(\xi, \eta, \tau) + \nu^*(z)\psi(\xi, \eta, \tau)^*$ with ψ solution of Eq. (1.30), and separate terms weighting ψ and ψ^* in Eq. (1.33), we end up with the coupled equations

$$\begin{aligned} +i\partial_\zeta \mu + \kappa\mu + a_0^2 \Gamma(\mu + \nu) &= 0 \\ -i\partial_\zeta \nu + \kappa\nu + a_0^2 \Gamma(\mu + \nu) &= 0. \end{aligned} \quad (1.34)$$

Simple arguments lead to the conclusion that an exponentially growing solution such that $u, v, \epsilon \propto \exp(\gamma z)$ with $\gamma = \sqrt{-\kappa(\kappa + 2\chi a_0^2)}$ does exist: given a pump beam in Kerr medium (either focusing or defocusing) there exist X-waves that get amplified along propagation. Their spectrum is given by Eq. (1.30) and plotted in figure 1.3. In a focusing (defocusing) medium the am-

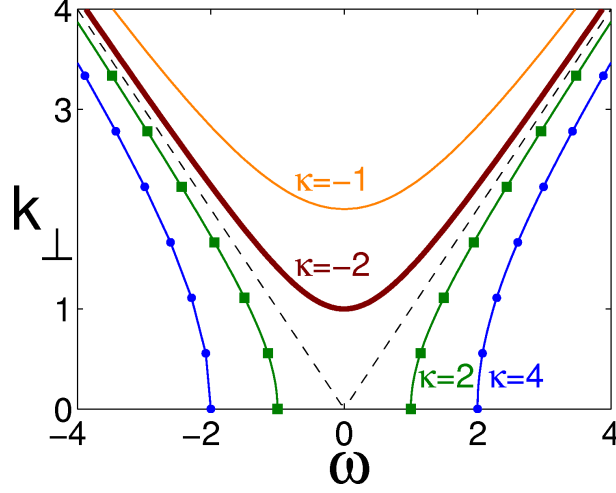


Fig. 1.3 Spatio-temporal spectrum for different X-waves ψ_κ . The dashed line is the spectrum of the simplest X-wave ($\kappa = 0$).

plication range involves $-2a_0^2 < \kappa < 0$ ($0 < \kappa < 2aa_0^2$). In figure 1.4 two examples of X-waves with different κ are given.

This simple perturbative analysis is confirmed by the numerical simulation of Eq. (1.2), which is reported in figure (1.5), and involve the early stage of propagation (i.e. it is limited to samples with dimension of the order the diffraction length) of a Gaussian beam with

$$A(x, y, z = 0) = \sqrt{I_0} \exp \left[- \left(\frac{x^2 + y^2}{2W_0^2} \right) - \left(\frac{t^2}{2T_p^2} \right) \right],$$

whose FWHM spot-size and duration (i.e. measured at “full width at half maximum” of the intensity profile) are $70\mu\text{m}$ and 100 fs , respectively. The other parameters are as follows: $n_0 = 1.5$, $n_{2I} = 2.5 \times 10^{-20}$; $k'' = 360 \times 10^{-28}$ in MKSA units, and the peak power is $P = 1.5P_c$, with $P_c = (0.61\lambda)^2\pi/(8n_{2I}n_0) \cong 2.6\text{ MW}$ the critical power for self-focusing [15].

The reported arguments are limited to a perturbative analysis, and deal with a beam which is essentially a pump wave, with a small superimposed “X-wave halo” (see [15] and also [79] for quadratic media). This halo can be clearly evident in the experiments and in the simulations, because it slowly decays far from the beam center. However experimentally investigated regimes involve dramatic reshaping processes whose analysis must be tackled with a different approach as discussed below.

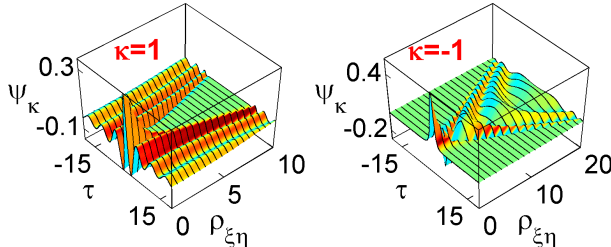


Fig. 1.4 Profiles of the X-waves ψ_κ for $\Delta = 1$ and $\kappa = \pm 1$ ($\rho_{\xi\eta}^2 = \xi^2 + \eta^2$).

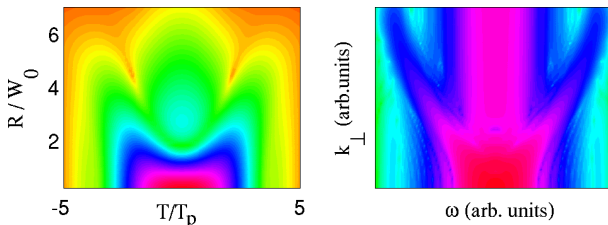


Fig. 1.5 Spatio-temporal intensity profile (left-panel) and spectral content (right-panel) of a Gaussian pulsed beam after the propagation in a nonlinear Kerr medium (parameters in the text).

1.5 THE NONLINEAR X-WAVE EXPANSION

We observe that X-waves are localized objects that exist even for a vanishing nonlinear response. Conversely, in the field of nonlinear wave propagation, SW are known as non-perturbative solutions that do not exist in absence of nonlinearity and for which a straightforward perturbative expansion (i.e. in power series of the relevant nonlinear coefficient, as e.g. n_{2I}) does not apply (see e.g. [80]). In this respect NLX, for which perturbative expansions are meaningful, are strikingly different from SW. In particular with simple argument one can arrive at the following interesting conclusion [16]: *if the pulsed-beam incident on a nonlinear sample is an X-wave, the nonlinearity just “dresses” the linear X-waves.* In other words, the nonlinearity does not destroy the propagation-invariant nature of X-waves. Additionally, even in the case for which the input beam is not an X-wave, but rather undergoes a negligible diffraction and dispersion (to some extent the incident beam approximates a propagation-invariant pulsed beam), then an X-wave is generated. Notably enough this result is not limited to a perturbative regime.

Indeed by re-writing our starting model (1.2) as

$$i\partial_z A + \frac{1}{2k} \nabla_{\perp}^2 A - \frac{k''}{2} \partial_t^2 A = \chi \mathcal{P}_{NL}(z, t, r), \quad (1.35)$$

where $\mathcal{P}_{NL}(z, t, r)$ is a nonlinear source, weighed by the coefficient χ ; one finds, after a straightforward expansion of A in powers of χ , that the relevant equation has still the form of Eq. (1.35) at any order in χ , where the RHS stems from the solutions at lower order. If $\chi\mathcal{P}_{NL}(z, t, r) = \mathcal{P}(t - \bar{\beta}z, r)$, the evolution according to Eq. (1.35) always provides a spatio-temporal spectrum corresponding to an X-wave [Eq. (1.9)]. Thus, if an X-wave is taken as the solution of the linear model ($\chi = 0$), the nonlinearity plays the role of “dressing” that solution, assuring that it continues to exist. Since this result is valid at any order in χ , it turns out that linearly-self-invariant beams are very robust against the nonlinearity, even beyond first order perturbation.

1.5.1 Some examples

(i) *X-waves propagating in a nonlinear medium.* \mathcal{P} can be interpreted as a function of the X-wave field and its complex conjugate, and travels unchanged, since it depends on $t - \beta z$:

(ii) *Harmonic generation.* this entails a polarization \mathcal{P} which is some power of the pump beam, traveling at the group velocity of the fundamental frequency; if diffraction and dispersion of the pump (in the absence of nonlinearity) is negligible, then $\mathcal{P} = \mathcal{P}(T - k'_P z, r)$, where k'_P is the inverse group velocity of the pump

(iii) *Kerr media.* Eq. (1.2) holds; for the solution at the lowest order ($n_{2I} = 0$), it is possible to take either an X wave-packet A_X centered around $\bar{\beta}$ (so that we fall in the case (i)); or a wide pulsed beam with negligible diffraction and dispersion (with $\bar{\beta} = 0$) (as in the case (ii) above). Higher orders are obtained in the form (1.35): at the first order the RHS is proportional to $A_X^2 A_X^*$. As a result of the following analysis, the correction to A_X is still a progressive undistorted wave traveling at the same velocity. At the next order in χ the situation is the same, and the same argument applies, leading to conclude that an X-wave is obtained again.

We can summarize by saying that whenever the polarization \mathcal{P} can be approximated as a function of a retarded time $t - \bar{\beta}z$ only, an X-wave emerges after the propagation in a nonlinear sample, at any order of the nonlinear effects.

1.5.2 Proof

By writing A , as a superposition of slash-X-waves,

$$A = \int_0^\infty \int_{-\infty}^\infty C(\alpha_1, \beta_1, z) J_0(\sqrt{k k''} \alpha_1 r) e^{-i(\alpha_1 + \beta_1/k'')(t - \beta_1 z)} d\alpha_1 d\beta_1, \quad (1.36)$$

and inserting Eq. (1.36) into Eq. (1.35), we find

$$i \frac{\partial C}{\partial z} - \frac{\beta^2}{2k''} C = \mathcal{X}_/[P](\alpha, \beta) e^{i(\alpha + \beta/k'')(\bar{\beta} - \beta)z}, \quad (1.37)$$

with (α, β) related to (ω, k_\perp) through Eqs. (1.18), and

$$\mathcal{X}_/[P](\alpha, \beta) = k\alpha \mathcal{B}[P] \left(\alpha + \frac{\beta}{k''}, \sqrt{k k''} \alpha \right). \quad (1.38)$$

Eq. (1.37) can be readily integrated by taking $C = 0$ at $z = 0$, obtaining

$$C(\alpha, \beta, z) = -i \mathcal{X}_/[P] \frac{\sin(gz)}{g} \exp\left\{i \left[\left(\alpha + \frac{\beta}{k''} \right) (\bar{\beta} - \beta) - \frac{\beta^2}{4k''} \right] z\right\}, \quad (1.39)$$

with

$$g = \frac{1}{2} \left[\left(\alpha + \frac{\beta}{k''} \right) (\bar{\beta} - \beta) + \frac{\beta^2}{2k''} \right]. \quad (1.40)$$

Eq. (1.39) can be interpreted in the (ω, k_\perp) , or (α, β) , planes and shows that, for large propagation distances, C tends to a Dirac δ centered at $g = 0$. Therefore the propagation acts as a spatio-temporal filter, selecting specific combinations of frequencies and wave-vectors that correspond to the condition $g = 0$, or explicitly in the (ω, k_\perp) plane

$$\frac{k''}{2} \left(\omega - \frac{\bar{\beta}}{k''} \right)^2 - \frac{k_\perp^2}{2k} = \frac{\bar{\beta}^2}{2k''}. \quad (1.41)$$

This curve represent an hyperbola, as sketched in figure 1.6. It is apparent that Eq. (1.41) is the dispersion relation corresponding to Eq. (1.8), and hence the resulting pulsed beam is a progressive undistorted wave traveling at inverse differential velocity $\bar{\beta}$.

1.5.3 Evidences

In the experimental results reported so far, there is a clear evidence of this hyperbola in the spectral domain, see e.g. [7, 55], as well as of a structured spectrum,[78, 81] that corresponding to the splitting phenomenon described in the following. The asymptotes over which energy is concentrated correspond to slash and backslash X-waves. Thus, in any nonlinear process which can be reduced to Eq. (1.35), X-wave-packets are spontaneously generated. In the case $\bar{\beta} = 0$ Eq. (1.41) yields the exact X-shaped spectrum. The specific features will in general depend on the source spectrum [16].

The previous argument supports the existence and the spontaneous formation of nonlinear X-waves. However an element is still missing: exact solutions. So far no analytic solutions are known for NLX, but numerical analysis can be applied as described below.

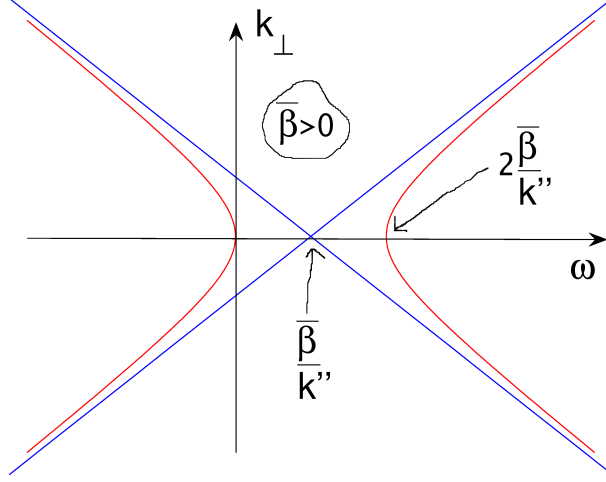


Fig. 1.6 Sketch of the generated spatio-temporal spectrum (symmetrized for $k_{\perp} < 0$) when $\bar{\beta} > 0$. The straight lines are slash and backslash spectra.

1.6 NUMERICAL SOLUTIONS FOR NONLINEAR X-WAVES

Nonlinear X-waves are found as solution to nonlinear wave equations. Let us consider again the normalized Eq. (1.29)

$$i\partial_{\zeta}u + \partial_{\xi}^2u + \partial_{\eta}^2u - \partial_{\tau}^2u + \Gamma|u|^2u = 0. \quad (1.42)$$

NLX with velocity $1/k'$ ($\beta = 0$) have the form $u = w(\xi, \eta, \tau) \exp(-i\beta_{\zeta}\zeta)$ with the real valued profile w satisfying the equation

$$\beta_{\zeta}w + \partial_{\xi}^2w + \partial_{\eta}^2w - \partial_{\tau}^2w + \Gamma w^3 = 0. \quad (1.43)$$

The number of parameters in the previous equation can be further reduced by introducing an additional rescaling that discriminates between the case $\beta_{\zeta} = 0$ and $\beta_{\zeta} \neq 0$, respectively. In the latter case, we set $v \equiv |\beta_{\zeta}|^{1/2}\tau$, $\gamma \equiv \Gamma/|\beta_{\zeta}|$, $b \equiv \beta_{\zeta}/|\beta_{\zeta}|$, and limiting to circularly symmetric solutions $w = f(\rho, v)$ that depend on $\rho = |\beta_{\zeta}|^{1/2}\rho_{\xi\eta} = [|\beta_{\zeta}|(\xi^2 + \eta^2)]^{1/2}$, we find

$$bf + \frac{1}{\rho} \frac{\partial f}{\partial \rho} + \frac{\partial^2 f}{\partial \rho^2} - \frac{\partial^2 f}{\partial v^2} + \gamma f^3 = 0 \quad (1.44)$$

where $b = \text{sign}(\beta_{\zeta})$. Eq. (1.44) holds true also in the case $\beta_{\zeta} = 0$, with $b = 0$, $\gamma = \Gamma$, $v \equiv \tau$ and $\rho = \rho_{\xi\eta}$. Both the families of NLX depend on the single parameter γ .

The degree of arbitrariness hidden by boundary conditions on f is removed by imposing $f(\rho, \pm\infty) = f(\infty, v) = 0$ and $\frac{df}{d\rho}(0, v) = 0$, which give a localized

solutions in 3D. We also fix the additional constraint $\max(f) = 1$, which does not limit the generality since it can be always satisfied by the free parameter I_0 in the normalization leading to Eq. (1.29).

Finding numerically X-waves solutions of Eq. (1.44) is a non-trivial task because of the slowly decaying tails in the radial (ρ) direction. A trick that can be used consists in interpreting Eq. (1.44) as an evolution problem in the ρ variable. In fact, by making a suitable discretization in the v coordinate, one reduces the original problem to a set of coupled equations in the variable ρ that can be solved by standard ODE algorithms (care is needed at the first step at $\rho = 0$ where boundary conditions must be used to avoid singularities). The v discretization can be done using pseudo-spectral techniques like Chebichev polynomials or “FFT” (we employed both the techniques and found comparable performances).

It turns out that if an appropriate guess is given for the field at $\rho = 0$, the numerical code provides a slowly decaying field with respect to v at any ρ . Conversely, a wrong guess furnishes an exploding solutions as ρ increases. By such an approach the richness of the nonlinear X-waves solutions can be simply unveiled, without resorting to shooting or iterative techniques, that result in computationally expensive and ill-conditioned problems. We found that an effective guess is given by the real or the imaginary part of the linear exact X-wave solution (which is a solution as $\gamma = 0$):

$$u = \frac{1}{\sqrt{(\Delta - iv)^2 + \rho^2}} \quad (1.45)$$

where Δ is a length scale with respect to v for the profile at $\rho = 0$. The real (imaginary) part provide an even (odd) profile at $\rho = 0$, which is inherited by the nonlinear solutions as discussed below (we take $\Delta = 1$ in the following). Once a solution for $\gamma \neq 0$ is found for a given set of parameters, we enlarged the integration domain to the maximum dimensions made available by our computational resources to verify that the function is indeed localized. In practice this amounts to increasing the maximum value of ρ in our ODE solver, and to enlarge the domain in v to avoid boundary effects in the ρ evolution.

1.6.1 Bestiary of solutions

A trial classification. Once the guess at $\rho = 0$ is fixed, the solution depends on two parameters b and γ . An open issue is the classification of nonlinear X-waves. For the moment they can be roughly divided into two classes, distinguished by the two values $b = 0$ and $b = 1$. The former correspond to spatio-temporal spectrum in low intensity regime (i.e., $\gamma \rightarrow 0$) lying around the spectral lines $k_\rho^2 = k_v^2$ (with obvious notation). Conversely the latter is characterized by $k_\rho^2 - k_v^2 = b$ and hence the spectrum in the low intensity limit is not contiguous to the origin. As a result the beam profile exhibits

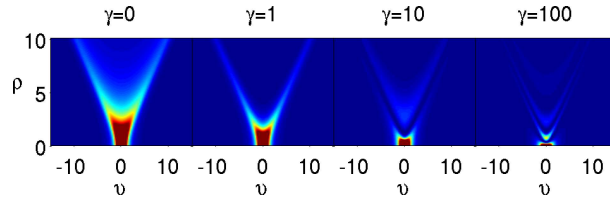


Fig. 1.7 “Dressing” of the fundamental even X-wave for an increasing nonlinearity: the intensity f^2 is shown Vs ρ and v ($\Delta = 1, b = 0$).

oscillations regardless of the value of γ , at variance with the case $b = 0$ where such oscillations appear at large values of γ (see figures in the following).

Infinite (non-numerable) number of solutions. Notably NLX exist both for focusing and defocusing nonlinearities (the latter case being relevant for BEC), as due to the fact that linear solutions exist; additionally it is well expected that the infinity of solutions in the linear case reflects into an infinity of solutions in the nonlinear case. In other words, differently from SW, which only exist in the presence of a nonlinear response and such that only one solution exist for a fixed set of parameters (e.g. waist), X-waves are not-numerable. A rigorous proof of this fact is still to come.

Infinite energy. Even if numerically the energy is necessarily finite (as the spatial grid adopted in the calculation), it is well established that Eq. (1.44) does not admit finite energy solutions [82]. Additionally, given the fact that the tails in any direction must decay according to the linear equation, because of the corresponding small values of $|u|^2$ so that the nonlinear terms are negligible, the numerical solution slowly decays with respect to ρ , and hence the NLX found numerically have infinite energy (for $\rho \in [0, \infty)$ and $v \in (-\infty, \infty)$).

Focusing nonlinearity. In figure 1.7 we show the effect of the nonlinear response on the profile of the fundamental X-wave (1.45). We consider the case $b = 0$, such that Eq. (1.45) is an exact solution for $\gamma = 0$ (in the absence of nonlinearity). Then we report the X-wave profile obtained numerically for increasing positive γ (focusing medium). It is clearly evident that the nonlinearity concentrates the energy around the central spot, up to a region at high γ where oscillations start to take place. Figure 1.8 displays the same result for odd X-waves. Figure 1.9 and 1.10 show solutions with $b = 1$, which display oscillations also in the linear regime ($\gamma = 0$), with frequency increasing with γ . The 3D representations of these numerical solutions are reported in figures 1.11 and 1.12.

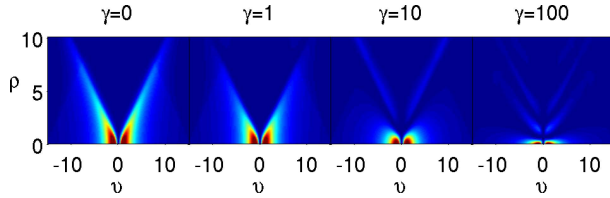


Fig. 1.8 “Dressing” of the fundamental odd X-wave for an increasing nonlinearity: the intensity f^2 is shown Vs ρ and ν ($\Delta = 1, b = 0$).

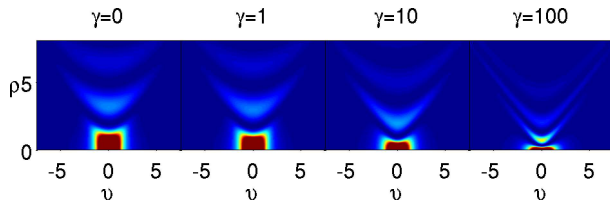


Fig. 1.9 “Dressing” of the fundamental even X-wave with $b = 1$ for an increasing nonlinearity: the intensity f^2 is shown Vs ρ and ν ($\Delta = 1, b = 1$).

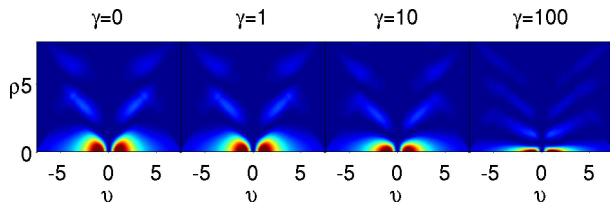


Fig. 1.10 “Dressing” of the fundamental even X-wave with $b = 1$ for an increasing nonlinearity: the intensity f^2 is shown Vs ρ and ν ($\Delta = 1, b = 1$).

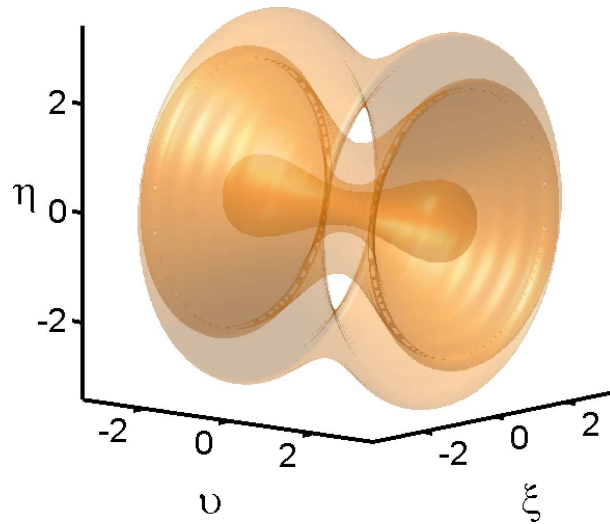


Fig. 1.11 Isosurface (at level 0.01 of u^2) of the even NLX solution with parameters: $\gamma = 100, b = 0, \Delta = 1, \kappa = 0$. Note that this kind of solution can be viewed as multiple fundamental X-waves nested one into the other.

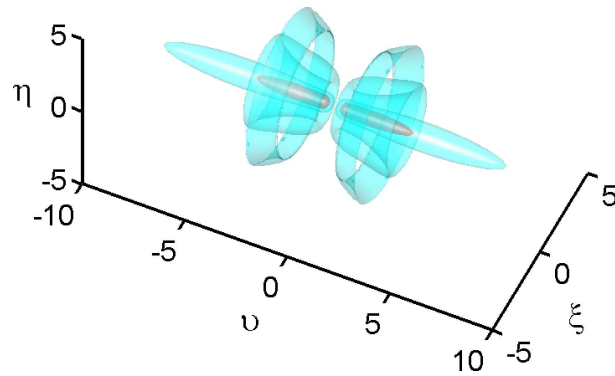


Fig. 1.12 Isosurface of the odd NLX solution with parameters ($\gamma = 100, b = 1, \Delta = 1, \kappa = 0$); the red surface corresponds to level 0.06 of u^2 and the cyan surface to level 0.014 of u^2 . This kind of X-waves is formed by symmetric bullets that travel locked together (high intensity area in the middle surface, in red) in the presence of an X-wave halo.

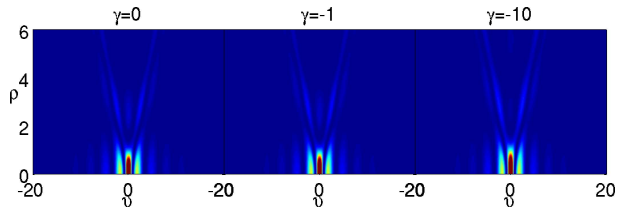


Fig. 1.13 “Dressing” of the even X-waves in Eq. (1.32) with $\kappa = \Delta = 1$ and $b = 0$ for an increasing defocusing nonlinearity.

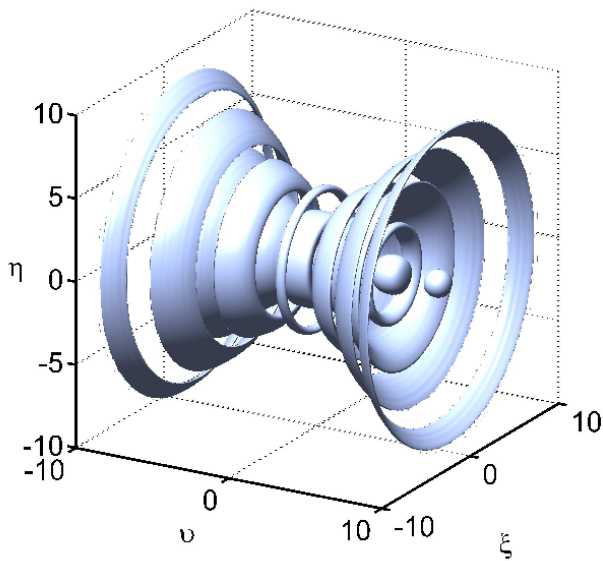


Fig. 1.14 Isosurface (u^2 , level 0.001) for an X-wave in a defocusing medium with parameters: $b = 1, \kappa = 1, \Delta = 1, \gamma = -1$. Note both the radial and the longitudinal modulation of the energy distribution which are due to non-vanishing κ and b parameters. This kind of solutions can be regarded as distributions of bullets (clearly evident at $\rho = 0$) with a modulated X-wave halo.

Defocusing nonlinearity. The situation for the defocusing case ($\gamma = -1$) is more tricky. This case is of particular interest for the matter X-waves, as discussed above. We consider only solution with even profile at $\rho = 0$. In the case $b = 0$ we were not able to find localized solutions starting from the guess given by Eq. (1.45). Conversely, results with this guess when $b = 1$ are obtained but, at variance with the focusing case, we were only able to find solutions up to some critical value of $|\gamma|$ ($|\gamma| \cong 2$). Nevertheless, using a different guess, namely the “ κ -X-wave” from Eq. (1.32) with $\kappa = 1$, solutions are found also for $b = 0$ and for higher values of $|\gamma|$, as displayed in figure 1.13. We observe that in the defocusing case solutions gets less localized as the amount of nonlinearity is increased (as physically reasonable). In figure 1.14 we show a 3D representation of a NLX in the defocusing case.

A remark. The reported examples are clearly not conclusive. Although, there is a numerical evidence of the existence of nonlinear X-wave solutions, their multitude and complexity calls for an analytical approach. So far the existence of NLX solutions can be only inferred from the regularity of the reported solutions but cannot be envisaged for shure.

1.7 COUPLED X-WAVE THEORY

Exact NLX solutions describe a stationary regime, i.e. a 3D bullet of energy (or density for BEC) traveling without distortion. However NLX may spontaneously generate during nonlinear propagation, and this is an highly dynamic process that, in some experimentally and numerically investigated cases, does not result into a propagation invariant regime. Indeed, it has been observed that even if an X-shaped spectrum is obtained, this does not necessarily correspond to a stable X-shaped packet, but to a periodical redistribution of energy in and out of a conical region [51, 55, 49]. This kind of behavior leads to consider nonlinear dynamics of X-waves.

In order to fix the ideas, one can take into account one or more X-waves spontaneously generated and then exhibiting some dynamics, or some X-wave generator device (i.e. an axicon) shooting X-waves into a nonlinear medium, inside which they interact (an experiment that, so far, has not been performed). In all these cases the natural approach is to develop a “coupled X-wave theory,” which is briefly reviewed in the following (for details see Ref. [16]).

We consider again Eq. (1.2), with $X(\alpha, \beta, z) = f_p(\alpha)C(\beta, z)$ being the X-wave transform of the solution A , which represents an X-wave-packet centered around the medium group velocity, i.e. $\bar{\beta} = 0$. If C is peaked around $\bar{\beta} = 0$, all components travel nearly at the same velocity, and one obtains the *coupled*

X-wave equations in the approximate form:

$$i\partial_z C(\beta, z) - \frac{\beta^2}{2k''} C(\beta, z) = -\frac{k n_{2I}}{n_0} \int \chi(\beta + \beta_1 - \beta_2 - \beta_3) C(\beta_1) C(\beta_2) C(\beta_3)^* d\vec{\beta}, \quad (1.46)$$

where the interaction kernel $\chi(\gamma)$ is the Fourier transform of the quantity $\sigma(s)$ defined below. Taking the Fourier transform of Eq. (1.46) [see Eq. (1.24)] we find

$$i\frac{\partial c}{\partial z} + \frac{k''}{2} \frac{\partial^2 c}{\partial s^2} + k_0 n_{2I} \sigma(s) |c|^2 c = 0. \quad (1.47)$$

Hence *the evolution of an X wave-packet in a nonlinear Kerr medium can be approximated by an effective 1+1D nonlinear Schrödinger equation with a non-homogeneous nonlinear coefficient*. The latter, given by $\sigma(s)$, has the dimensions of an inverse area, and is expressed by the Fourier transform of the kernel χ :

$$\sigma(s) = 4\pi^2 k'' \int_{-\infty}^{\infty} \chi(\gamma) e^{i\gamma s/k''} d\gamma = \int_0^{\infty} |2\pi\sqrt{k''} \varphi_j^{(p)}|^4 r dr. \quad (1.48)$$

$\sigma(s)$ is the spatial self-overlap of the component X-wave profile at $\beta = 0$. Any solution c of the nonlinear Eq. (1.47), with C given by Eq. (1.24), generates a solution A of the envelope equation (1.2)

$$A = \int C(\beta, z) \psi_j^{(p)}(r, t - \beta z, \beta) d\beta = \int c(s, z) \xi_j^{(p)}(r, t, s, z) ds, \quad (1.49)$$

with

$$\xi_j^{(p)}(r, t, s, z) = \frac{1}{\sqrt{k''}} \int e^{-i(s+t)\frac{\beta}{k''} + i\frac{\beta^2}{k''} z} \varphi_j^{(p)}(r, t - \beta z) d\beta. \quad (1.50)$$

Thus the 3D+1 nonlinear evolution problem (1.2) reduces (under suitable approximations) to a 1+1D model (1.47). Two applications are discussed below.

1.7.1 Fundamental X-wave/Fundamental soliton

Let us consider the previous results for the fundamental X-shaped profile [see Eq. (1.27)]. It can be found that $\sigma(s)$ is a bell-shaped function [16]; when the on-axis temporal dynamics is dominated by the c envelope (i.e. the temporal width of c is smaller than Δ), it can be approximated by $\sigma(0) \cong W_0^{-2}$, where W_0 is the spatial beam waist. The effective nonlinear Schrödinger equation

can be rewritten as

$$i \frac{\partial c}{\partial z} + \frac{k''}{2} \frac{\partial^2 c}{\partial s^2} + \frac{k_0 n_{2I}}{W_0^2} |c|^2 c = 0, \quad (1.51)$$

so that the effective nonlinear coefficient has, compared with the plane-wave coefficient, the additional factor W_0^{-2} . This reflects the compensation of diffraction owing to the X-waves, which behave as “modes of free space”. $\sigma(s)$ resembles the mode-overlap in a waveguide from coupled mode theory. Eq. (1.51) is well known from soliton theory and a number of non-trivial exact solutions can be built (see e.g. [80]). The fundamental soliton [when $\sigma(s) \cong \sigma(0)$] can be expressed in terms of the peak c_0^2 of the energy distribution function; it reads

$$A = \int c_0 \left(\sqrt{\frac{c_0^2 k_0 n_{2I} \sigma(0)}{k''}} s \right) \exp[i \frac{c_0^2 k_0 n_{2I} \sigma(0)}{2} z] \xi_j^{(0)}(r, t, z, s) ds. \quad (1.52)$$

Eq. (1.52) expresses the “dressing” mechanism associated with the nonlinearity: the latter acts only on the shape of the envelope which, even in the linear limit, would travel almost undistorted. In spite of this remarkable difference with solitary waves, the (approximate) validity of an integrable model such as Eq. (1.51) seems to establish a strong link with solitons.

1.7.2 Splitting and replenishment in Kerr media as an higher order soliton

The self-trapped behavior of the 3D beam, given by Eq. (1.52) is ultimately related to the X-shape. More interesting dynamics can be described referring to multi-soliton solutions of the integrable Eq. (1.51). The $N > 1$ solitons (see e.g. [83, 80]) are natural concepts in explaining splitting and replenishment, investigated numerically in [49] and experimentally in [52]. Noteworthy, breathing linear X-waves have been reported [28, 25]. Using higher order soliton solutions for (1.51), (see e.g. [83]) one can build approximate *breathing nonlinear X-wave* [16]. Figure 1.15 shows an example of the corresponding spatio-temporal profile. The periodic depletion and replenishment of the X-shaped distribution is apparent. During the propagation, breather-solution pulsates and the beam evolves retaining most of its energy localized, but exhibiting the non-trivial nonlinear dynamics of the X-wave. It is also noticeable that higher order solitons exhibit the spectral splitting typically described in numerical simulations.

Before concluding, it is fruitful to summarize the picture of the splitting/replenishment phenomenon, commonly observed in experiments in Kerr media, in terms of NLX. At the beginning a wide bell-shaped pulsed beam evolves into an X-wave, owing to the spatio-temporal pattern formation of X-wave instability [15]. Once the envelope width is sufficiently reduced, the

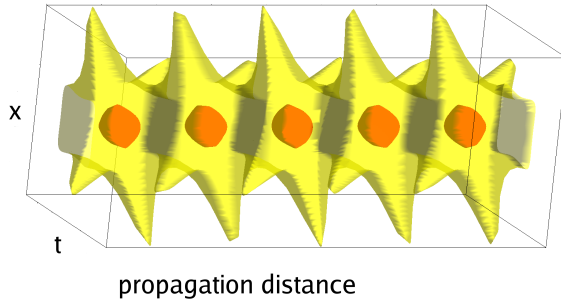


Fig. 1.15 Typical spatio-temporal profile (at $y = 0$) of a breathing X-wave. Two isosurfaces are displayed: the darkest (red) corresponds to higher intensity.

increased intensity through compression feeds the generation of a higher order soliton, or breather. After some spatio-temporal oscillations, several mechanisms may intervene to stop the periodic behavior, e.g. losses (eventually of nonlinear origin, such as two-photon absorption) or simply that, for large propagation distances, the nonlinear response average out due to the sliding between components of the finite energy X wave-packet.

1.8 A BRIEF REVIEW OF EXPERIMENTS

1.8.1 Angular dispersion

The key feature that identifies X-waves is the angular dispersion (AD), i.e. the dependence of the temporal frequency on angle. Using AD it is possible to moderate, and in principle make vanishing any tendency to delocalize energy due to material dispersion [19, 84, 85, 86, 87]. Before explicitly invoking X-waves, the role of AD was considered with the aim of obtaining “broad-band phase-matching” in SHG experiments [88]. Nowadays, AD is adopted in all modern commercial optical-parametric amplifiers, that exploit second order nonlinearity to achieve tunable light sources; a very active field of research, linking together localized waves and laser physics [10, 89, 90, 91, 92, 31]. AD was also exploited for the observation of temporal solitons in quadratic media [93].

1.8.2 Nonlinear X-waves in Quadratic media

The experiments leading to the first observation of NLX were aimed at the generation of light bullets starting from a Gaussian pulse displaying AD, in order to compensate the group velocity difference between two harmonics (a first harmonic FH and a second harmonic SH) that get involved in the

nonlinear process. During these experiments, it was found that AD-free input beams lead to unexpected spatio-temporal localization. Numerical simulations showed the emergence of an X-type structure, and the results were explained by the existence of a stationary nonlinear X-wave acting as an attractor for the nonlinear dynamics [5, 6, 12]. The reported observations were then confirmed by more accurate experiments, that ultimately lead to the “spatio-temporal tomography” of the generated nonlinear X-wave [9, 8]. Related experimental results, with emphasis on the conical emission processes, were recently reported in [94, 95, 96].

1.8.3 X-waves in self-focusing of ultra-short pulses in Kerr media

Recent investigations of ultra-short pulse propagation in Kerr media with normal ($k'' > 0$) dispersion [49, 51, 33, 52, 53, 97, 54, 55] have shown that light filaments formed in condensed matter have conical oscillating tail [51] and a complicated spatio-temporal structure [52]. Numerical simulations [49, 50] show that the dynamics is governed by cycles of pulse splitting and subsequent temporal replenishment of the on-axis pulse. Past the first splitting point the field pattern shows evidence of X waves. Since the latter is highly dynamical the X features are best seen in the spectral domain (spectrally resolved far field) where the wave exhibits characteristic tails that follow the X-shaped dispersion curve (see Fig. 1.6). In typical experimentally retrieved spectra, X-shaped tails are clearly evident (as e.g. [55, 98]). The observed spectral arms are due to conical emission [75, 99, 15], the corresponding arms follow the asymptotic lines $k_{\perp} = \sqrt{k_0 k''}(\omega - \omega_0)$ characteristic of the linear dispersion relationship (see Fig. 1.6), while at low spatial frequencies ($k_{\perp} \cong 0$) there is the evidence of the predicted spectral gap [55]; indeed the locus of points θ, Ω corresponding to maximum intensity in the arms fits with the hyperbolic curve of Eq. (1.41) [16]. The splitting and replenishment scenario is well settled (qualitatively, to say the least) in the higher order soliton proposed above. These results provide a clear indication that NLX can be taken as a “paradigm” for interpreting ultra-fast dynamics of laser pulses in condensed matter, however many issues are still to be deepened.

1.9 CONCLUSION AND DEVELOPMENTS

In this chapter we provided an introduction to the rapidly growing field of NLX, from which many other lines of investigation recently originated, as due to the intense research activity in modern photonics. Mostly related to this manuscript are the “O-waves” (the analogous of envelope X-waves but with anomalous dispersion), including nonlinear effects [56, 34]; as well as the deepening of 2+1D models [70, 29].

Fields which are still at an embryonic stages, but that are potentially very productive are NLX of discrete models [32, 35] and in dissipative systems (like optical resonators) [37, 38, 36].

Many results are currently being published that concern LW and NLX in photonic crystals, i.e. media displaying a periodic refractive index, see the other chapters in this book and [39, 40, 41, 42, 43, 44, 46, 47].

In the authors' opinion the most relevant challenges, from a theoretical perspectives, are certainly those related in finding exact solutions for NLX. For what concerns experiments perhaps the most fascinating issue is the observation of *matter X-waves*, while a lot of interesting investigations are still to be performed in nonlinear optics. First of all those related to many theoretical predictions, and then topics like harmonic generation by an X-wave and the nonlinear interaction between LW and related issues. A particular mention goes to quantum effects (as in [100, 101, 102]), which are relevant for both Matter- and Optical-X-waves; the interplay between squeezing and entanglement due to nonlinear processes and 3D+1 propagation invariant properties is still largely un-explored and may have relevant implications in fundamental physics and quantum information.

References

1. Trillo, S. and Torruellas, W., editors (2001). *Spatial solitons*. Springer-Verlag, Berlin.
2. Kivshar, Y. and Agrawal, G. P. (2003). *Optical solitons*. Academic Press, New York.
3. Malomed, B. A., Mihalache, D., Wise, F., and Torner, L. (2005). Spatiotemporal optical solitons. *J. Opt. B: Quantum Semiclassical Opt.*, 7:R53–R72.
4. Wise, F. and Di Trapani, P. (2002). Spatiotemporal solitons: the hunt for light bullets. *Opt. Photon. News*, pages 28–32.
5. Valiulis, G., Kilius, J., Jedrkiewicz, O., Bramati, A., Minardi, S., Conti, C., Trillo, S., Piskarskas, A., and Di Trapani, P. (2001). Space-time nonlinear compression and three dimensional complex trapping in normal dispersion. In *Quantum Electronics and Laser Science Conference*, volume 57 of *Trends in Optics and Photonics*. Optical Society of America, Washington, D.C. Postdeadline Papers QPD10-1, [arXiv:physics/311081](https://arxiv.org/abs/physics/311081).
6. Conti, C., Di Trapani, P., Trillo, S., Valiulis, G., Minardi, S., and Jedrkiewicz, O. (2002). Nonlinear x-waves:light bullets generation in normally dispersive media? In *Quantum Electronics and Laser Science Conference*, Trends in Optics and Photonics, page QTuJ6. Optical Society of America, Washinton,D.C.
7. Kriger, K. (2003). Bullets of light. *Phys. Rev. Focus*, 12. Story 7 (<http://focus.aps.org/story/v12/st7>).
8. Trull, J., Jedrkiewicz, O., Trapani, P. D., Matijosius, A., Varanavicius, A., Valiulis, G., Danielius, R., Kucinskas, E., Piskarskas, A., and Trillo, S. (2004). Spatiotemporal three-dimensional mapping of nonlinear x waves. *Phys. Rev. E*, 69:026607.
9. Jedrkiewicz, O., Trull, J., Valiulis, G., Piskarskas, A., Conti, C., Trillo, S., and Trapani, P. D. (2003). Nonlinear x waves in second-harmonic generation: Experimental results. *Phys. Rev. E*, 68:026610.

10. Orlov, S., Piskarskas, A., and Stabinis, A. (2002). Focus wave modes in optical parametric generators. *Opt. Lett.*, 27:2103–2105.
11. Trillo, S., Conti, C., Trapani, P. D., Jedrkiewicz, O., Trull, J., Valiulis, G., and Bellanca, G. (2002). Colored conical emission by means of second-harmonic generation. *Opt. Lett.*, 27:1451–1453.
12. Di Trapani, P., Valiulis, G., Piskarskas, A., Jedrkiewicz, O., Trull, J., Conti, C., and Trillo, S. (2003). Spontaneously generated x-shaped light bullets. *Phys. Rev. Lett.*, 91:093904.
13. Conti, C., Trillo, S., Valiulis, G., Piskarskas, A., Jedrkiewicz, O., Trull, J., and Di Trapani, P. (2003). Nonlinear electromagnetic x-waves. *Phys. Rev. Lett.*, 90:170406. ArXiv:physics/0204066.
14. Conti, C. and Trillo, S. (2003). X-waves generated at the second harmonic. *Opt. Lett.*, 28:1251–1253. arXiv:physics/0208097.
15. Conti, C. (2003). X-wave-mediated instability of plane waves in kerr media. *Phys. Rev. E*, 68:016606.
16. Conti, C. (2004). Generation and nonlinear dynamics of x waves of the schr[o-umlaut]dinger equation. *Phys. Rev. E*, 70:046613.
17. Porras, M. A., Trillo, S., Conti, C., and Di Trapani, P. (2003). Paraxial envelope x-waves. *Opt. Lett.*, 28:1090–1092.
18. Porras, M. A. and Trapani, P. D. (2004). Localized and stationary light wave modes in dispersive media. *Phys. Rev. E*, 69:066606. arXiv:physics/0309084v1.
19. Porras, M. A., Valiulis, G., and Di Trapani, P. (2003). Unified description of bessel x waves with cone dispersion and tilted pulses. *Phys. Rev. E*, 68:016613.
20. Longhi, S. (2004). Spatio-temporal gauss-laguerre in dispersive media. *Phys. Rev. E*, 68:066612.
21. Ciattoni, A., Conti, C., and Di Porto, P. (2004). Universal space time properties of x-waves. *J. Opt. Soc. Am. A*, 21:451–455.
22. Ciattoni, A., Conti, C., and Di Porto, P. (2004). Vector electromagnetic x waves. *Phys. Rev. E*, 69:036608.
23. Ciattoni, A. and Di Porto, P. (2004). One-dimensional nondiffractive pulses. *Phys. Rev. E*, 69:056611.
24. Saari, P. and Reivelt, K. (2004). Generation and classification of localized waves by lorentz transformations in fourier space. *Phys. Rev. E*, 69:036612.

25. Zamboni-Rached, M., Shaarawi, A. M., and Recami, E. (2004). Focused x-shaped pulses. *J. Opt. Soc. Am. A*, 21:1564–1574. [arXiv:physics/0309098v1](#).
26. Zamboni-Rached, M., Hernandez-Figueroa, H. E., and Recami, E. (2004). Chirped optical x-shaped pulses in material media. *J. Opt. Soc. Am. A*, 21:2455–2463. [arXiv:physics/0405059v2](#).
27. Grunwald, R., Keibel, V., Griebner, U., Neumann, U., Kummrow, A., Rini, M., Nibbering, E. T. J., Piché, M., Rousseau, G., and Fortin, M. (2003). Generation and characterization of spatially and temporally localized few-cycle optical wave packets. *Phys. Rev. A*, 67:063820.
28. Shaarawi, A. M., Besieris, I. M., and Said, T. M. (2003). Temporal focusing by use of composite x-waves. *J. Opt. Soc. Am. A*, 20:1658–1665.
29. Kominis, Y., Moshonas, N., Papagiannis, P., Hizanidis, K., and Christodoulides, D. (2005). Continuous-wave-controlled nonlinear x-wave generation. *Opt. Lett.*, 30:2924–2926.
30. Longhi, S. (2004). Parametric amplification of spatiotemporal localized envelope waves. *Phys. Rev. E*, 69:016606.
31. Butkus, R., Orlov, S., Piskarskas, A., Smilgevičius, V., and Stabinis, A. (2005). Phase matching of optical x-waves in nonlinear crystals. *Opt. Commun.*, 244:411–421.
32. Droulias, S., Hizanidis, K., Meier, J., and Christodoulides, D. (2005). X-waves in nonlinear normally dispersive waveguide arrays. *Opt. Express*, 13:1827–1832.
33. Porras, M. A., Parola, A., Faccio, D., Dubietis, A., and Trapani, P. D. (2004). Nonlinear unbalanced bessel beams: Stationary conical waves supported by nonlinear losses. *Phys. Rev. Lett.*, 93:153902.
34. Porras, M. A., Parola, A., and Di Trapani, P. (2005). Nonlinear unbalanced o waves: nonsolitary conical light bullets in nonlinear dissipative media. *J. Opt. Soc. Am. B*, 22:1406–1416.
35. Kevrekidis, P. G., Gagnon, J., Frantzeskakis, D. J., and Malomed, B. A. (2006). X,y,z-waves: Extended structures in nonlinear lattices. [arXiv:cond-mat/0603397](#).
36. Staliunas, K. and Tlidi, M. (2005). Hyperbolic transverse patterns in nonlinear optical resonators. *Phys. Rev. Lett.*, 94:133902.
37. Soto-Crespo, J. M., Grellu, P., and Akhmediev, N. (2006). Optical bullets and "rockets" in nonlinear dissipative systems and their transformations and interactions. *Opt. Express*, 14:4013–4025.

38. Zhou, C. T., Yu, M. Y., and He, X. T. (2006). X-wave solutions of complex ginzburg-landau equations. *Phys. Rev. E*, 73:026209.
39. Christodoulides, D. N., Efremidis, N. K., Di Trapani, P., and Malomed, B. A. (2004). Bessel x-waves in 2d and 3d bidispersive optical systems. *Opt. Lett.*, 29:1446–1448.
40. Longhi, S. and Janner, D. (2004). X-shaped waves in photonic crystals. *Phys. Rev. B*, 70:235123.
41. Longhi, S. and Janner, D. (2004). Diffraction and localization in low-dimensional photonic bandgaps. *Opt. Lett.*, 29:2653–2655.
42. Longhi, S., Janner, D., and Laporta, P. (2004). Propagating pulsed bessel beams in periodic media. *J.Opt.B: Quantum Semiclass.Opt.*, 6:477–481.
43. Longhi, S. (2005). Localized and nonspreading spatiotemporal wannier wave packets in photonic crystals. *Phys. Rev. E*, 71:016603.
44. Manela, O., Segev, M., and Christodoulides, D. N. (2005). Nondiffracting beams in periodic media. *Opt. Lett.*, 30:2611–2613.
45. Polesana, P., Faccio, D., Di Trapani, P., Dubietis, A., Piskarskas, R., Varanavicius, A., Gaizauskas, A., and Piskarskas, A. (2005). High localization, focal depth and contrast by means of nonlinear besses beams. *Opt. Express*, 13:6110.
46. Staliunas, K. and Herrero, R. (2006). Nondiffractive propagation of light in photonic crystals. *Phys. Rev. E*, 73:016601.
47. Staliunas, K., Serrat, C., Herrero, R., Cojocar, C., and Trull, J. (2006). Subdiffractive light pulses in photonic crystals. *Phys. Rev. E*, 74:016605.
48. Bergé, L., Germaschewski, K., Grauer, R., and Rasmussen, J. J. (2002). Hyperbolic shock waves of the optical self-focusing with normal gvd. *Phys. Rev. Lett.*, 89:153902.
49. Kolesik, M., Wright, E. M., and Moloney, J. V. (2004). Dynamics nonlinear x-waves for femtosecond pulse propagation in water. *Phys. Rev. Lett.*, 92:253901. ArXiv:physics/0311021.
50. Kolesik, M., Wright, E. M., and Moloney, J. V. (2005). Interpretation of the spectrally resolved far field of femtosecond pulses propagating in bulk nonlinear dispersive media. *Opt. Express*, 13:10729–10741.
51. Dubietis, A., Gaizauskas, E., Tamosauskas, G., and Trapani, P. D. (2004). Light filaments without self-channeling. *Phys. Rev. Lett.*, 92:253903.
52. Matijosius, A., Trull, J., Di Trapani, P., Dubietis, A., Piskarskas, R., Varanavicius, A., and Piskarskas, A. (2004). Nonlinear space-time dynamics of ultrashort wave packets in water. *Opt. Lett.*, 29:1123–1125.

53. Faccio, D., Matijosius, A., Dubietis, A., Piskarskas, R., Varanavicius, A., Gaizauskas, E., Piskarskas, A., Couairon, A., and Trapani, P. D. (2005). Near- and far-field evolution of laser pulse filaments in kerr media. *Phys. Rev. E*, 72:037601.
54. Couairon, A., Gaizauskas, E., Faccio, D., Dubietis, A., and Trapani, P. D. (2006). Nonlinear x-wave formation by femtosecond filamentation in kerr media. *Phys. Rev. E*, 73:016608.
55. Faccio, D., Porras, M. A., Dubietis, A., Bragheri, F., Couairon, A., and Di Trapani, P. (2006). Conical emission, pulse splitting, and x-wave parametric amplification in nonlinear dynamics of ultrashort light pulses. *Phys. Rev. Lett.*, 96:193901.
56. Porras, M., Dubietis, A., Kucinskas, E., Bragheri, F., Couairon, A., Faccio, D., and Di Trapani, P. (2005). From x- to o-shaped spatiotemporal spectra of light filaments in water. *Opt. Lett.*, 30:3398–3400.
57. Conti, C. and Trillo, S. (2004). Nonspreading wave packets in three dimensions formed by an ultracold bose gas in an optical lattice. *Phys. Rev. Lett.*, 92:12040. ArXiv:physics/0308051.
58. Anderson, M. H., Ensher, J. R., Matthews, M. R., Wieman, C. E., and Cornell, E. A. (1995). Observation of bose-einstein condensation in a dilute atomic vapor. *Science*, 269:198–201.
59. Davis, K. B., Mewes, M. O., Andrews, M. R., van Druten, N. J., Durfee, D. S., Kurn, D. M., and Ketterle, W. (1995). Bose-einstein condensation in a gas of sodium atoms. *Phys. Rev. Lett.*, 75:3969–3973.
60. Dalfovo, F., Giorgini, S., Pitaevskii, L., and Stribngari, S. (1999). Theory of bose-einstein condensation in trapped gases. *Rev. Mod. Phys.*, 71:463–512.
61. Khaykovich, L., Schreck, F., Ferrari, G., Bourdel, T., Cubizolles, J., Carr, L., Castin, Y., and Salomon, C. (2002). Formation of a matter-wave bright solitons. *Science*, 296:1290–1293.
62. Pitaevskii, L. (1996). Dynamics of collapse of a confined bose gas. *Phys. Lett. A*, 221:14–18.
63. Bergé, L. (2000). Stability criterion for attractive bose-einstein condensates. *Phys. Rev. A*, 62:23607.
64. Saito, H. and Ueda, M. (2003). Dynamically stabilized bright solitons in a 2d bose-einstein condensate. *Phys. Rev. Lett.*, 90:40403.
65. Anderson, B. P. and Kasevich, M. (1998). Macroscopic quantum interference from atomic tunnel arrays. *Science*, 282:1686–1689.

66. Ostrovskaya, E. A. and Kivshar, Y. (2003). Matter-wave gap solitons in atomic band-gap structures. *Phys. Rev. Lett.*, 90:160407.
67. Burger, S., Cataliotti, F. S., Fort, C., Minardi, F., Inguscio, M., Chiofalo, M. L., and Tosi, M. P. (2001). Superfluid and dissipative dynamics of a bose-einstein condensate in a periodic optical potential. *Phys. Rev. Lett.*, 86:4447–4450.
68. Pötting, S., Meystre, P., and Wright, E. M. (2003). Atomic solitons in optical lattices. In Slusher, R. and Eggleton, B., editors, *Nonlinear photonic crystals*, volume 10 of *Photonics*, page 301. Springer.
69. Moloney, J. and Newell, A. (2003). *Nonlinear Optics*. Westview Press, New York.
70. Larsen, P. V., Sorensen, M. P., Bang, O., Krolikowski, W. Z., and Trillo, S. (2006). Nonlocal description of x waves in quadratic nonlinear materials. *Phys. Rev. E*, 73:036614.
71. Carusotto, I., Embriaco, D., and LaRocca, G. C. (2002). Nonlinear atom optics and bright-gap-soliton generation in finite optical lattices. *Phys. Rev. A*, 65:R053611.
72. Saari, P. (2001). Superluminal localized waves of electromagnetic field in vacuo. Printed in: *Time’s Arrows, Quantum Measurement and Superluminal Behavior*, Scientific Monographs: Physics Sciences Series, Italian CNR Publ. Rome, 2001, pp. 37-48, [arXiv:physics/0103054](https://arxiv.org/abs/physics/0103054).
73. Lu, J. and Liu, A. (2000). An x wave transform. *IEEE Trans. Ultrason., Ferroelect., Freq. Contr.*, 47:1472–1480.
74. Salo, J. and Salomaa, M. M. (2001). Orthogonal x waves. *J. Phys. A: Math. Gen.*, 34:9319–9327.
75. Liou, L. W., Cao, X. D., McKinstrie, C. J., and Agrawal, G. P. (1992). Spatiotemporal instabilities in dispersive nonlinear media. *Phys. Rev. A*, 46:4202–4208.
76. Luther, G. G., Newell, A. C., Moloney, J. V., and Wright, E. M. (1994). Short-pulse conical emission and spectral broadening in normally dispersive media. *Opt. Lett.*, 19:789–791.
77. Kosareva, O. G., Kandidov, V. P., Brodeur, C. Y., A. adn Chien, and Chin, S. L. (1997). Conical emission from laser-plasma interactions in the filamentation of powerful ultrashort laser pulses in air. *Opt. Lett.*, 22:1332–1334.
78. Nibbering, E. T. J., Curley, P. F., Grillon, G., Prade, B. S., France, M. A., Salin, F., and Mysyrowicz (1996). Conical emission from self-guided femtosecond pulses in air. *Opt. Lett.*, 21:62–64.

79. Longhi, S. (2004). Localized subluminal envelope pulses in dispersive media. *Opt. Lett.*, 29:147–149.
80. Drazin, P. G. and Johnson, R. S. (1989). *Solitons: An Introduction*. Cambridge University Press.
81. Faccio, D., Di Trapani, P., Minardi, S., Bramati, A., Bragheri, F., Liberale, C., Degiorgio, V., Dubietis, A., and Matijosius, A. (2004). Far-field spectral characterization of conical emission and filamentation in kerr media. [arXiv:physics/0405086v1](https://arxiv.org/abs/physics/0405086v1).
82. Berge, L. (1998). Wave collapse in physics: principles and applications to light and plasma waves. *Phys. Rep.*, 286:259–370.
83. Agrawal, G. (2001). *Nonlinear Fiber Optics*. Academic Press, New York, 3 edition.
84. Martinez, O. E. (1986). Pulse distortions in tilted pulse schemes for ultrashort pulses. *Opt. Comm.*, 59:229–232.
85. Orlov, S., Piskarskas, A., and Stabinis, A. (2002). Localized optical sub-cycle pulses in dispersive media. *Opt. Lett.*, 27:2167–2169.
86. Szatmari, S., Simon, P., and Feuerhake (1996). Group-velocity-dispersion-compensated propagation of short pulses in dispersive media. *Opt. Lett.*, 21:1156–1158.
87. Sonajalg, H., Ratsep, M., and Saari, P. (1997). Demonstration of the bessel-x pulse propagating with strong lateral and longitudinal localization in a dispersive media. *Opt. Lett.*, 22:310–312.
88. Szabo, G. and Bor, Z. (1990). Broadband frequency doubler for femtosecond pulses. *Appl. Phys. B*, 50:51–54.
89. Danielius, R., Piskarskas, A., Di Trapani, P., Andreoni, A., Solcia, C., and Foggi, P. (1996). Matching of group velocities by spatial walk-off in collinear three-wave interaction with tilted pulses. *Opt. Lett.*, 21:973–975.
90. Trull, J., Jedrkiewicz, O., Di Trapani, P., Matijosius, A., Varanavicius, A., Valiulis, G., Danielius, R., Kucinskas, E., Piskarskas, A., and Trillo, S. (2004). Spatiotemporal three-dimensional mapping of nonlinear x waves. *Phys. Rev. E*, 69:026607.
91. Di Trapani, P., Andreoni, A., Banfi, G. P., Solcia, C., Danielius, R., Piskarskas, A., Foggi, P., Monguzzi, M., and Sozzi, C. (1995). Group-velocity self-matching of femtosecond pulses in noncollinear parametric generation. *Phys. Rev. A*, 51:3164–3168.
92. Di Trapani, P., Andreoni, A., Foggi, P., Solcia, C., Danielius, R., and Piskarskas (1995). Efficient conversion of femtosecond blues pulses by

- travelling-wave parametric generation in non-collinear phase matching. *Opt. Commun.*, 119:327–332.
93. Di Trapani, P., Caironi, D., Valiulis, G., Dubietis, A., Danielius, R., and Piskarskas, A. (1998). Observation of temporal solitons in second-harmonic generation with tilted pulses. *Phys. Rev. Lett.*, 81:570–573.
94. Zeng, H., Wu, K., Xu, H., and Wu, J. (2005). Seeded amplification of colored conical emission via spatiotemporal modulational instability. *Appl. Phys. Lett.*, 87:061102.
95. Zeng, H., Wu, J., Xu, H., and Wu, K. (2006). Generation and weak beam control of two-dimensional multicolored arrays in a quadratic nonlinear medium. *Phys. Rev. Lett.*, 96:083902.
96. Su, W., Qian, L., Luo, H., Fu, X., Zhu, H., Wang, T., Beckwitt, K., Chen, Y., and Wise, F. (2006). Induced group-velocity dispersion in phase-mismatched second-harmonic generation. *J. Opt. Soc. Am. B*, 23:51–55.
97. Faccio, D., Di Trapani, P., Minardi, S., Bramati, A., Bragheri, A., Bragheri, F., Liberale, C., Degiorgio, V., Dubietis, A., and Matijosius (2005). Far-field spectral characterization of conical emission and filamentation in kerr media. *J. Opt. Soc. Am. B*, 22:862–869.
98. Liu, J., Schroeder, H., Chin, S. L., Li, R., Yu, W., and Xu, Z. (2005). Space-frequency coupling, conical waves, and small-scale filamentation in water. *Phys. Rev. A*, 72:053817.
99. Luther, G. G., Newell, A. C., and Moloney, J. V. (1994). The effects of normal dispersion on collapse events. *Physica D*, 74:59–73.
100. Saari, P., Menert, M., and Valtna, H. (2005). Photon localization barrier can be overcome. *Opt. Commun.*, 246:445–450.
101. Conti, C. (2004). Quantum x-waves in kerr media and the progressive undistorted squeezed vacuum. [arXiv:quant-ph/0409130](https://arxiv.org/abs/quant-ph/0409130).
102. Conti, C. (2003). Generation of entangled 3d localized quantum wavepackets via optical parametric amplification. [arXiv:quant-ph/0309069](https://arxiv.org/abs/quant-ph/0309069).